Compartmentalized and Binary Behavior of Terminal Dendrites in Hippocampal Pyramidal Neurons

Dong-Sheng Wei,[1] Yan-Ai Mei,[1] Ashish Bagal,[2] Joseph P. Y. Kao,[2,3] Scott M. Thompson,[2] Cha-Min Tang[1,2]*

The dendritic arbor of pyramidal neurons is not a monolithic structure. We show here that the excitability of terminal apical dendrites differs from that of the apical trunk. In response to fluorescence-guided focal photolysis of caged glutamate, individual terminal apical dendrites generated cadmium-sensitive all-or-none responses that were subthreshold for somatic action potentials. Calcium transients produced by all-or-none responses were not restricted to the sites of photolysis, but occurred throughout individual distal dendritic compartments, indicating that electrogenesis is mediated primarily by voltage-gated calcium channels. Compartmentalized and binary behavior of parallel-connected terminal dendrites can greatly expand the computational power of a single neuron.

Dendrites are not passive antennae that simply receive synaptic inputs but actively process and transform inputs as they are received (*1–5*). The apical dendritic arbor can be divided into three morphologically distinct regions, the thick main apical trunk, a set of short intermediate branches, and a set of long, thin terminal branches (*6*). The apical trunk of pyramidal cell dendrites is relatively thick and contains sufficient densities of sodium channels to mediate forward and backward propagation of action potentials (*7*). Terminal branches, in contrast, have diameters one-fourth that of the apical trunk and do not decrease over distance (*8*). Terminal dendritic segments constitute 70 to 90% of the combined length of the apical dendritic arbor (*6*). Despite being the main recipient of excitatory synaptic inputs, little is known about the passive and active transformations an individual terminal segment performs on its inputs.

The impedance mismatch between the thin truncated terminal dendrite and its parent branch creates conditions favoring electrical compartmentalization (*9–11*). Electrical compartmentalization of dendritic segments enables groups of inputs to be bound together in a dynamic manner that depends on the temporal and spatial coherence of the inputs. If terminal dendrites were also to express sufficiently high densities of voltage-gated conductances, their outputs might switch readily between two discrete states (*10*). Such bistable behavior would enable nonlinear and binary logical operations. These predictions remain untested, because it has not been possible to record from a terminal dendrite or to restrict synaptic activation over a wide dynamic range to a single branch.

We used fluorescence-guided focal photolysis of caged glutamate (*12, 13*) and whole-cell recording from CA1 pyramidal cells in 2- to 3-week-old organotypic hippocampal slice cultures (*14, 15*). A confocal reconstruction of one representative neuron from this preparation is shown in Fig. 1A, illustrating the large numbers of long, thin terminal branches arising from the thick, gradually tapering apical trunk.

Terminal and proximal dendrites responded in qualitatively different manners (Fig. 1B). Strong stimulation of first- or second-order apical dendrites reliably elicited regenerative sodium and calcium action potentials. In contrast, identical stimulation of terminal dendritic segments elicited only lower amplitude, plateau-shaped all-or-none depolarizations, and was unable to elicit propagated action potentials.

Terminal oblique branches contribute a significant portion of the CA1 dendritic arbor. Photostimulation directed at these branches was also able to generate all-or-none responses (Fig. 1C). At low photostimulus strength, the response amplitude varied proportionally to the pulse duration and decayed with a monotonic time course. At some threshold level, photostimulation resulted in a sharp transition from graded responses to plateau-like all-or-none responses. Further increases in stimulus strength increased neither the amplitude nor the duration of the suprathreshold response. The mean amplitude (±SD) of the all-or-none depolarization was 8.7 ± 2.1 mV for terminal oblique branches that joined the main apical trunk within 175 μm of the soma (n = 31, V_m = −70 mV). The mean amplitude for terminal branches of the apical tuft that join the second- and third-order branches >350 μm from the soma was 8.5 ± 1.9 mV (n = 39). The mean duration of the all-or-none depolarization at half-maximal amplitude was 208 ± 38 ms and 268 ± 55 ms for the oblique and apical tuft terminal dendrites, respectively.

The amplitude, kinetics, and threshold of the suprathreshold dendritic response were voltage-dependent (Fig. 2, A and B). At relatively depolarized potentials, the kinetics of the responses was slow, but the threshold for all-or-none responses could be reached with low photostimulation strength. At more hyperpolarized potentials, the amplitude and decay rate increased, but greater stimulation strength was required to reach the transition threshold. The increased amplitude may result from increased driving force and from recruitment of T-type calcium channels that are inactivated at more depolarized membrane potentials. The increased kinetics of decay may result from the recruitment of hyperpolarization-activated current (I_h).

All-or-none responses were readily apparent in the presence of tetrodotoxin (TTX), and hence did not require voltage-dependent Na^+ conductances. The mean amplitude was 8.1 ± 1.0 mV before and 7.9 ± 1.0 mV after the addition of 1 μM TTX (n = 6). We therefore tested the effects of blocking voltage-dependent Ca^{2+} conductances with low concentrations of Cd^{2+} (25 μM). Cadmium had no observable effect on subthreshold responses, but greatly attenuated responses to stronger photostimuli (n = 9) (Fig. 2C). Cadmium eliminated a pulse-like component of the glutamate response. We conclude that the amplitude of the suprathreshold depolarization is not determined by the number of glutamate receptors activated by the stimulus, but rather by the number of voltage-gated calcium channels that are secondarily activated.

In neocortical basal dendrites, increases in cytoplasmic Ca^{2+} were localized to the site of photostimulation during the all-or-none response (*16*). To determine the degree of compartmentalization achieved in terminal apical dendrites, the spatial distribution of electrogenesis in apical dendrites was measured with calcium imaging (Fig. 3). Weak photostimuli produced small depolarizations and barely detectable calcium transients. Stronger but still subthreshold stimuli elicited localized calcium transients. In response to suprathreshold stimuli, however, calcium

[1]Departments of Neurology and [2]Physiology, University of Maryland School of Medicine, Baltimore, MD 21201, USA. [3]Medical Biotechnology Center, University of Maryland Biotechnology Institute, Baltimore, MD 21201, USA.

*To whom correspondence should be addressed. E-mail: ctang@som.umaryland.edu

transients appeared throughout an entire distal branch within the time resolution of a single 100-ms image acquisition window (rightmost panel in Fig. 3A).

The calcium transient associated with the suprathreshold dendritic depolarization stopped at the first branch point in all of the oblique branches (n = 11), and at the first or second proximal branch points in 10 of 12 apical tuft terminal dendrites (Fig. 3B). In the remaining two apical terminal dendrites, the Ca^{2+} signal ended before the first branch point. Because distinct calcium transients at sites up to 100 μm away from the site of photolysis could clearly be observed within a single 100-ms time window, we conclude that strong stimulation results in regenerative activation of voltage-dependent Ca^{2+} channels and that this electrogenesis is highly compartmentalized.

N-methyl-D-aspartate (NMDA) receptors are required for the initiation of the all-or-none dendritic response in both neocortical and hippocampal pyramidal cells. AP5 (100 μM) eliminated all-or-none responses, leaving a residual graded AMPA (α-amino-3-hydroxy-5-methyl-4-isoxazolepropionic acid) receptor–mediated current component (Fig. 4A) (n = 6). NBQX (6-nitro-7-sulfamoylbenzo[f]quinoxaline-2,3-dione) (100 μM) did not block the suprathreshold all-or-none response (Fig. 4B) (n = 5). As a further test of the relative importance of NMDA and AMPA receptors in initiating the suprathreshold response, experiments were carried out with caged NMDA (100 μM). Photolysis of caged NMDA consistently elicited suprathreshold all-or-none depolarizations (n = 10).

The nonexponential decay of the suprathreshold dendritic responses suggests that they are actively terminated by voltage-gated conductances. Several pharmacological manipulations were performed to test this hypothesis. We first examined the effects of extracellularly applied cesium (2 mM), a relatively specific blocker of I_h at this concentration (*17*). Cesium produced no appreciable change in subthreshold dendritic responses. At more hyperpolarized membrane potentials, however, cesium attenuated the afterhyperpolarization by 83% (n = 5) (Fig. 4C). We suggest that I_h is expressed in terminal dendritic segments and can contribute to the termination of the suprathreshold depolarization.

A more pronounced and qualitatively different effect was produced by increasing intracellular calcium buffering with BAPTA [1,2-bis(2-aminophenoxy)ethane-*N*,*N*,*N*′,*N*′-tetraacetic acid] (Fig. 4D). The duration of the plateau-shaped depolarization increased by 324 ± 46% over a 30-min period following the establishment of whole-cell recording with 10 mM BAPTA (n = 14). The amplitude of the response, however, was essentially unaffected. The response prolongation is most easily explained if calcium-activated potassium channels are expressed in terminal dendrites (*18*, *19*). BAPTA decreases intracellular free calcium and would thereby diminish their role in membrane repolarization. Increased calcium buffering may also attenuate calcium-dependent inactivation of dendritic calcium channels.

A major excitatory input to the apical

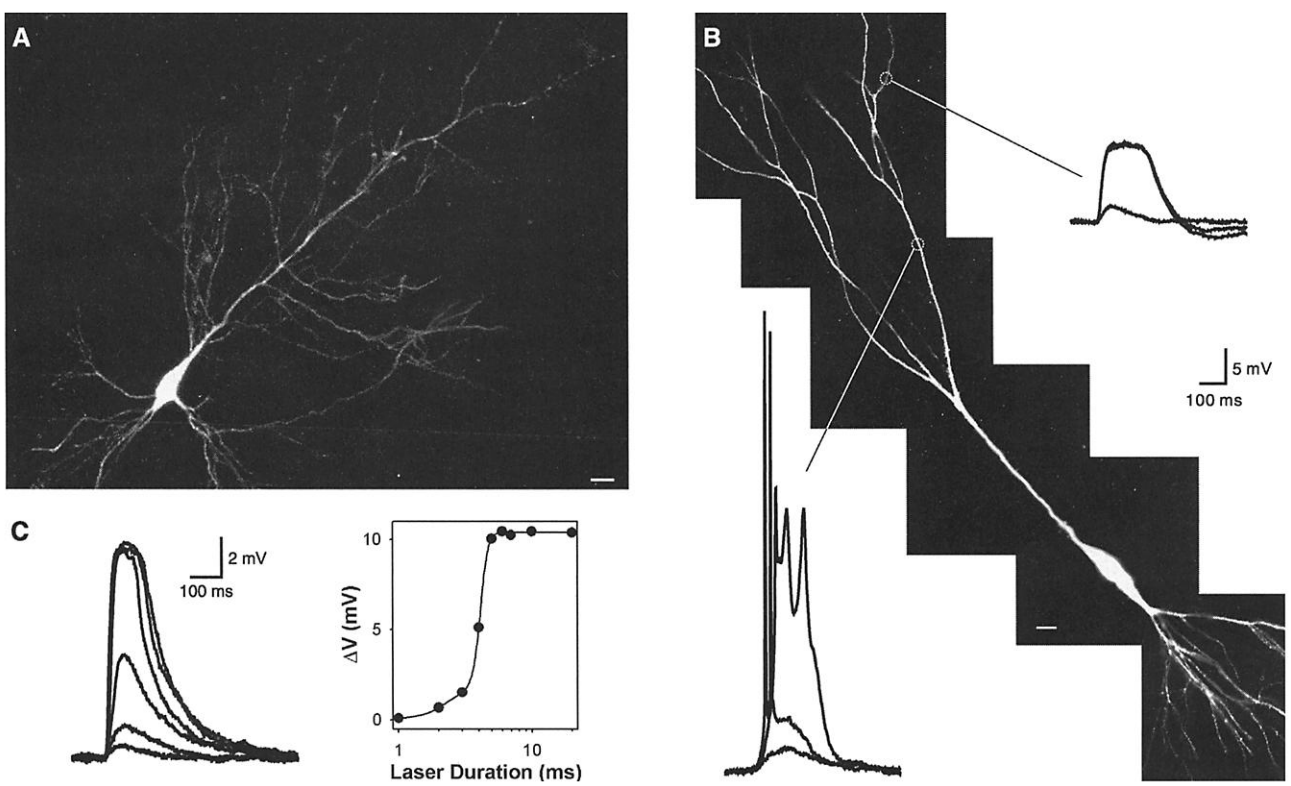

Fig. 1. Nonlinear input-output transfer characteristics of individual terminal dendrites. (**A**) Confocal reconstruction of a CA1 pyramidal cell in a hippocampal slice culture that was biolistically transfected with green fluorescent protein. Both primary and higher-order dendritic branches resemble those described for CA1 cells in acute hippocampal slices. Bar, 20 μm. (**B**) Focal photolysis of caged glutamate at two dendritic regions marked by the dotted circles of an Alexa 594–filled CA1 hippocampal pyramidal neuron. The voltage responses elicited with 4-, 10-, and 16-ms laser pulses are shown as recorded from the soma. Weak stimulation at either site elicited small graded depolarizations. Strong stimulation of the second-order apical dendrite resulted in fast action potentials. Strong stimulation of the individual terminal dendritic branch, in contrast, elicited all-or-none, plateau-like responses to the 10- and 16-ms laser pulses, but not fast action potentials. Because this montage of wide-field images was acquired with a high numerical aperture objective, thin terminal dendrites outside the plane of focus are not captured. Bar, 20 μm. Baseline V_m = −70 mV. (**C**) The input-output transfer function of a terminal apical tuft dendrite. Small graded depolarizations that were proportional to stimulus intensity were elicited in response to brief laser pulses ("subthreshold"). Small increases in the strength (pulse duration) of photostimulation resulted in a steep transition to larger responses of fixed maximal amplitude ("suprathreshold"). Baseline V_m = −70 mV.

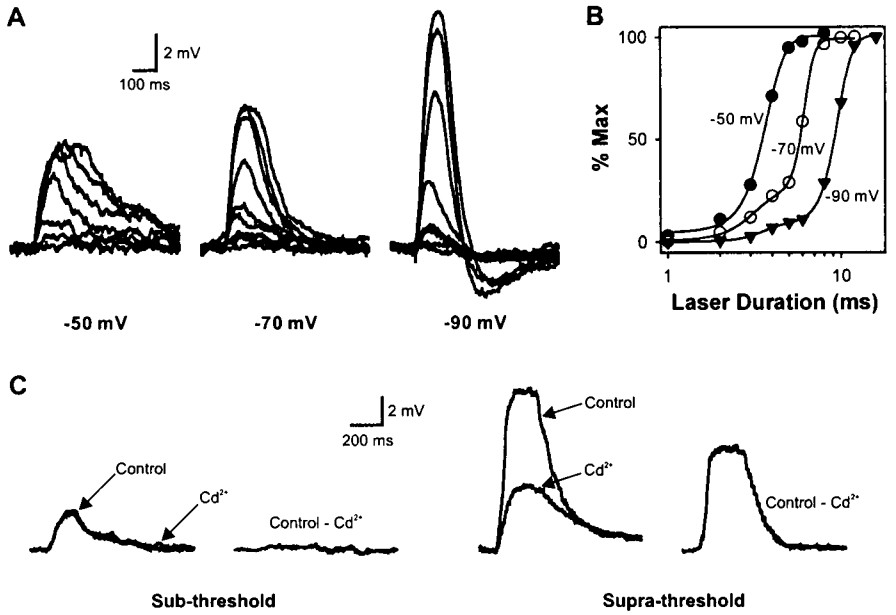

Fig. 2. Voltage-gated calcium channels underlie all-or-none terminal dendritic responses. (**A**) The transition between graded and all-or-none dendritic responses was voltage-dependent. A series of laser pulses of increasing duration was applied to a distal dendritic branch while polarizing the membrane potential in the presence of TTX and NBQX. (**B**) The threshold for all-or-none responses was reached with shorter laser pulses when elicited from the more depolarized potentials (●, –50 mV; ○, –70 mV; ▼, –90 mV). (**C**) A pulse-like component of the suprathreshold all-or-none response of distal dendrites was blocked by 25 μM Cd^{2+}, and thus mediated by voltage-dependent Ca^{2+} channels, whereas the graded subthreshold responses were unaffected. Baseline V_m = –70 mV.

dendrites of CA1 neurons are the Schaffer collaterals from CA3 neurons, which discharge in bursts of action potentials. Bursts of excitatory inputs enable NMDA receptor–mediated conductances to more effectively generate sustained dendritic depolarization (*20*). The strong photostimuli in these experiments mimic the results of coincident bursts of excitation at adjacent synapses. Indeed, intracellular recordings from CA1 neurons in vivo during CA3 burst discharges reveal a sustained monophasic voltage-dependent depolarization lasting about 100 ms, which may represent the in vivo correlate of suprathreshold terminal dendritic depolarizations (*21*).

Our study illustrates how the form of a dendritic structure can determine its function. We suggest that the amplitude of the suprathreshold response of a terminal dendrite is determined not by the number of synaptic receptors activated, but by its physical dimensions and the number of its voltage-gated channels. It may not be coincidental that the amplitudes of the suprathreshold depolarizations (coefficient of variation ≈ 0.2) and the length of the terminal apical dendrites both show a narrow distribution (*6*, *8*). Perhaps the physical dimensions of terminal dendrites have evolved to insure that somatic action potentials are not triggered by the suprathreshold response of a single terminal branch, but only when several branches are activated.

Our results also show that dendritic pro-

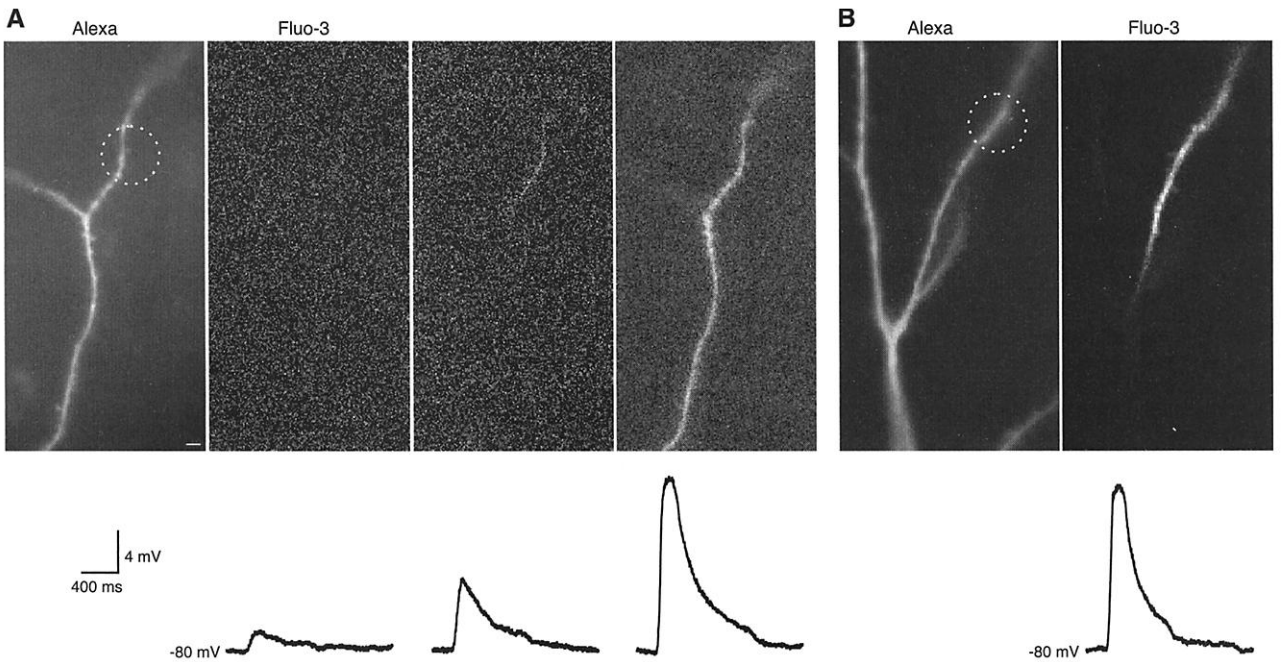

Fig. 3. Regenerative electrogenesis is confined to individual terminal branches. (**A**) An intermediate apical dendrite and its two daughter terminal dendrites were imaged using Alexa 594 optics (leftmost panel). Caged glutamate was photolyzed within the 10-μm-diameter spot marked by the dotted circle. Three pulses of increasing UV laser pulse duration were then delivered while imaging the resultant calcium transients using Fluo-3 filters. The electrical responses associated with the three UV pulses are shown below their respective calcium signals. The calcium transients are presented as the difference in the Fluo-3 signal in response to photolysis and the baseline fluorescence. Bar, 2.6 μm. (**B**) Intracellular Ca^{2+} transients associated with the all-or-none terminal dendritic response typically stopped abruptly at the first or second branch point, presumably because the depolarization of the distal branch failed to produce a suprathreshold depolarization of the intermediate dendrite. Diameter of UV illumination = 10 μm.

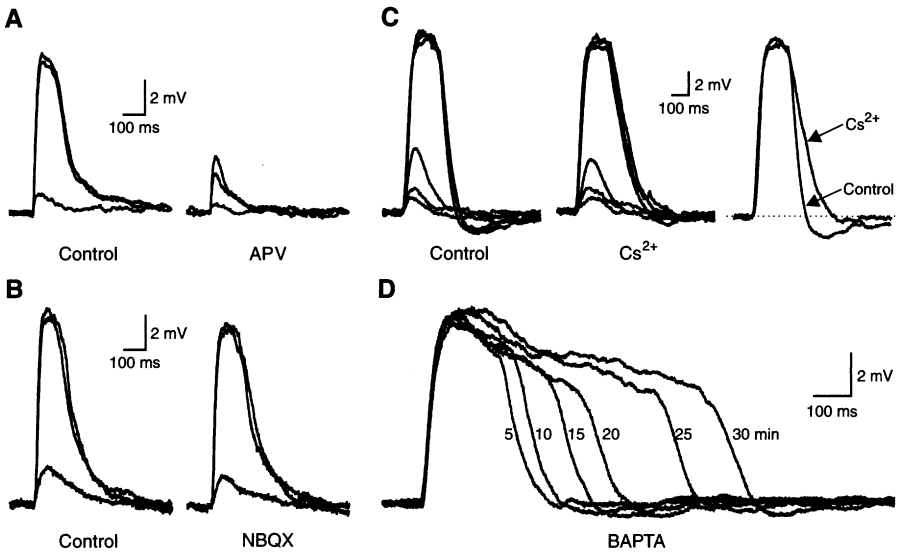

Fig. 4. Pharmacology of the suprathreshold terminal dendritic response. (**A**) Addition of APV (D,L-2-amino-5-phosphonovaleric acid; 100 μM) eliminated the suprathreshold depolarization leaving a residual AMPA receptor–mediated depolarization. Baseline V_m = –70 mV. (**B**) Addition of NBQX (100 μM) did not eliminate the suprathreshold depolarization. Baseline V_m = −70 mV. (**C**) Extracellular cesium (2 mM) had little effect on the subthreshold response, but prolonged the suprathreshold responses. A control and a cesium response to supramaximal stimulation are superimposed for comparison. Baseline V_m = −90 mV. (**D**) High concentrations of the calcium chelator BAPTA (10 mM) in the patch-pipette solution markedly prolonged the duration of the suprathreshold dendritic response, and the prolongation increased as a function of time. The numbers next to the individual traces mark the time in minutes following the initiation of whole-cell recording. NBQX is present. Baseline V_m = −70 mV.

cessing utilizes both graded and binary operations. The localized bistable behavior of terminal dendrites is well suited for nonlinear logical operations (*10*). The main apical trunk, in contrast, links the large number of terminal branches in parallel and is specialized for the rapid forward and backward propagation of action potentials. These complementary features would confer the dendritic arbor with parallel processing capabilities utilizing a large array of quasi-independent terminal dendrites with nonlinear signal processing capabilities and thus greatly expand the computational power of a single neuron.

References and Notes

1. M. Häusser, N. Spruston, G. J. Stuart, *Science* **290**, 739 (2000).
2. D. Johnston, J. C. Magee, C. M. Colbert, B. R. Christie, *Annu. Rev. Neurosci.* **19**, 165 (1996).
3. I. Segev, M. London, *Science* **290**, 744 (2000).
4. R. Yuste, D. W. Tank, *Neuron* **16**, 701 (1996).
5. J. Schiller, G. Major, H. J. Koester, Y. Schiller, *Nature* **404**, 285 (2000).
6. N. J. Bannister, A. U. Larkman, *J. Comp. Neurol.* **360**, 150 (1995).
7. N. Spruston, Y. Schiller, G. Stuart, B. Sakmann, *Science* **268**, 297 (1995).
8. M. Trommald, V. Jensen, P. Andersen, *J. Comp. Neurol.* **353**, 260 (1995).
9. I. Segev, W. Rall, *Trends Neurosci.* **21**, 453 (1998).
10. B. W. Mel, in *Dendrites*, G. Stuart, N. Spruston, M. Häusser, Eds. (Oxford Univ. Press, Oxford, 1999), pp. 271–289.
11. P. A. Rhodes, in *Cerebral Cortex* P. S. Ulinski, Ed. (Kluwer Academic/Plenum, New York, 1999), vol. 13, chap. 3.
12. C.-M. Tang, *Curr. Protoc. Neurosci.*, in press.
13. The 351- to 364-nm output of an argon ion laser or the output of a weak 532-nm targeting laser were launched into a 100-μm-diameter optical fiber. The exit end of the optical fiber is projected onto a conjugate of the field diaphragm plane along the epifluorescence path of the microscope with a relay lens system and a dichroic mirror. The relay lens system was designed to compensate for the chromatic aberration of the water-dipping objective so that the ultraviolet (UV) and visible illumination were focused on the same plane. It was also specifically designed to create a homogenously illuminated spot 10 to 12 μm in diameter rather than a small spot with a gaussian distributed light intensity. Cells were patch-clamped with pipettes containing the long-wavelength fluorescent dye Alexa 594 (100 μM) to allow visualization of the fine terminal branches with minimal inadvertent photolysis of the caged glutamate (γ-CNB-glutamate or *N*-Nmoc-glutamate) (*22*) or caged NMDA (β-CNB-NMDA). The light from the visible laser is used to "paint" the target site of photolysis without inducing photolysis or phototoxicity. The amount of free glutamate photoreleased was controlled by varying the UV laser pulse duration. Terminal dendritic segments arising either from the distal apical tuft or oblique branches were studied.
14. Hippocampal slice cultures were prepared from 5- to 7-day-old rat pups (*15*). After >14 days in vitro, whole-cell recordings were made from CA1 pyramidal cells using pipettes containing 135 mM KCH_3SO_3, 10 mM Hepes, 10 mM NaCl, 1 mM $MgCl_2$, 0.1 mM K_4BAPTA, 2 mM Mg^{2+}-ATP, and 10 mM phosphocreatine, buffered to pH 7.3 with KOH. Inclusion of 10 mM K_4BAPTA was compensated by reduction of KCH_3SO_3 to 100 mM. TTX (1 μM) was used in most experiments. Exceptions include results describe in Fig. 1, B and C. For Ca^{2+} imaging, no BAPTA was included in the pipette solution. The extracellular saline contained 145 mM NaCl, 3 mM KCl, 10 mM Hepes, 2 mM $CaCl_2$, 1 mM $MgCl_2$, 10 mM glucose, and 0.1 mM glycine. Trolox (250 to 500 μM) was included to reduce photooxidative damage. All experiments were performed at room temperature. Biolistic transfection of 12- to 14-day-old cultures with DNA encoding enhanced GFP was performed with the Helios Gene-gun (*23*). Cells were imaged with a confocal microscope 2 to 3 days after transfection.
15. B. H. Gähwiler, S. M. Thompson, E. Audinat, R. T. Robertson, in *Culturing Nerve Cells*, G. Banker, K. Goslin, Eds. (MIT Press, Cambridge, MA, 1991), pp. 379–411.
16. Fluo-3 was used as the calcium indicator, because it undergoes a large increase in fluorescence upon binding Ca^{2+} and because of its moderate K_d. Alexa Fluor 594 hydrazide was included in order to image the dendrites. A relatively high concentration of Fluo-3 (0.5 to 1 mM) was used to optimize detection of calcium transients in the thin terminal dendrites. Use of high concentrations of calcium indicators allows for more reliable detection of calcium influx (*24*), but slows the decay of the calcium transient. This strategy is well suited for these experiments, where spatial resolution is more important than temporal resolution. A back-thinned Quantix CCD (charge-coupled device) camera was used in conjunction with IPLab image acquisition software to capture the calcium transients.
17. G. Maccaferri, M. Mangoni, A. Lazzari, D. DiFrancesco, *J. Neurophysiol.* **69**, 2129 (1993).
18. J. C. Magee, in (*10*), pp. 139–160.
19. N. L. Golding, H. Y. Jung, T. Mickus, N. Spruston, *J. Neurosci.* **19**, 8789 (1999).
20. S. Hestrin *et al.*, *Cold Spring Harbor Symp. Quant. Biol.* **50**, 87 (1990).
21. A. Ylinen *et al.*, *J. Neurosci.* **15**, 30 (1995).
22. F. M. Rossi, M. Margulis, C.-M. Tang, J. P. Y. Kao, *J. Biol. Chem.* **272**, 32933 (1997).
23. A. K. McAllister, *Biolistic Transfection of Neurons*, Science's STKE (2000); http://stke.sciencemag.org/cgi/content/full/OC_sigtrans;2000/51/pl1.
24. E. Neher, G. J. Augustine, *J. Physiol.* **450**, 273 (1992).

25. We thank B. E. Alger, A. Keller, and P. Rhodes for their comments, and the U.S. Department of Veterans Affairs (C.-M.T.), NIH (C.-M.T. and J.P.Y.K.), and University of Maryland Bressler Fund (S.M.T.) for financial support.

30 March 2001; accepted 11 July 2001